Electronic Supplementary Material (ESI) for Journal of Materials Chemistry A. This journal is © The Royal Society of Chemistry 2024

Electronic Supplementary Material

AuPt nanostructures with a high Hydrogen Evolution Reaction activity through a halide-mediated microwave assisted route

Xuesong Zhang,[a] Jesús Chacón-Borrero,[b] Ren He,[b] Jaume Gázquez,[a] Miquel Torras,[a] Andreu Cabot,[b,c] Anna Roig,[a] and Pablo Guardia*[a]

[a] *Institut de Ciència de Materials de Barcelona (ICMAB-CSIC), Campus UAB, Bellaterra, 08193, Spain.*

[b] *Catalonia Institute for Energy Research (IREC), Sant Adrià de Besòs, Barcelona, 08930, Spain.*

[c] *ICREA, Pg. Lluis Companys, Catalonia, Barcelona, 08010, Spain.*

E-mail: pguardia@icmab.es

SUPPLEMENTARY INDEX

I-NCS CHARACTERIZATION

Fig. S1. Evolution of the NCs size and morphology as a function of time for the synthesis of $AuPt_{1/1}$. Samples were annealed at 160 °C in a solution containing a 1:1 Au:Pt molar ratio for (a) 10 s, (b) 30 s, (c) 1 min, (d) 2 min, (e) 5 min, and (f) 10 min.

Fig. S2. Evolution of the AuPt NCs size and shape as a function of the amount of PVP_{10K} (25, 50 and 100 mg) for different Au:Pt ratios.

Fig. S3. Evolution of the size and shape for AuPt NCs as a function of the total metal concentration (Au + Pt).

Fig. S4. XRD and UV-Vis patterns for AuPt NCs synthesized at different Au:Pt ratios without ($Au:Pt_{x/y}$; a, b) and with ($Au:Pt_{x/yCl}$ c, d) HCl.

Fig. S5. a) Comparison between the final Pt amount inside the NCs evaluated by ICP-OES (Pt_{ICP} in %) and the Pt amount added in solution ($Pt_{feeding}$ in %) for samples prepared under standard conditions (open blue circles) and in the presence of an excess of chlorine ions (green crosses). b) Evaluation of the difference in Pt content (ΔPt) between samples prepared with and without excess chlorine ions as a function of Pt content in the reaction solution ($Pt_{feeding}$ in %). The yellow area corresponds to the Pt % for the 1:6 to 1:2 Au:Pt ratio range.

Fig. S6. Size and shape evolution of AuPt NCs produced at different Au:Pt ratios (0:1 a-d; 1:4 e-h; 1:1 i-l; and 1:0: m-p) under different amounts of chlorine ions (0, 10, 20 and 50 µL of a 37 wt% HCl solution). Scale bar = 50 nm.

Fig. S7. Size and shape evolution as a function of PVP_{10k} amount (25, 50 and 100 mg) for AuPt NCs produced in the presence of 10 µL of chlorine ions. Scale bar = 50 nm.

Fig. S8. TEM images for AuPt NCs synthesized at 1:4 (a-c) and 1:1 (d-f) rations but increasing total metal concertation (2, 4 and 8 mM). In the reaction solution, 10 µL of an HCl solution (37 wt%) were added deliberately to increase the amount of chlorine ions. Scale bar = 50 nm.

Fig. S9. Direct comparison of AuPt NCs produced with a 1:1 Au:Pt molar ratio without or with HCl using a MW-assisted approach for 10 min (a, d) or an oil bath for 10 min (b, e) and 60 min. (c, f). Scale bar = 50 nm.

Fig. S10. a-c) TEM images of the NCs produced in three different experiments but under the same reaction conditions ($AuPt_{1/4Cl}$). d) TEM image of NCs produced after scaling up the reaction condition from 4 to 70 mL (17.5-fold). The final volume was the maximum possible achieved using the flexiWAVE reactor (Milestone™ Srl).

Fig. S11. FT-IR pattern of pure PVP_{10k}, $AuPt_{1/1}$ before and after PVP_{10k} removal.

Fig. S12. Electrocatalytic HER performance in 0.5 M H_2SO_4. LSV of the AuPt NCs synthesized in the absence (a) or presence (b) of chlorine without IR. (c) Comparison of the LSV with and without IR compensation (dashed and solid lines, respectively) for $AuPt_{1/4}$ and $AuPt_{1/4Cl}$ samples.

Fig. S13. Magnification of the Nyquist plot reported in Fig. 3h along with the equivalent circuit model.

Table S1. Summary of the specific data of the references cited in Fig. 3g.

Table S2. Summary of the parameters obtained from the RC equivalent circuit model.

II-HER MEASUREMENT IN NEUTRAL AND ALKALINE MEDIA

Fig. S14. LSV curves of Pt/C, $AuPt_{1/4}$, and $AuPt_{1/4Cl}$ in (a) 1 M potassium phosphate-buffered saline (PBS, pH=7) electrolyte and (b) 1 M potassium hydroxide (pH=14) electrolyte.

Table S3. Summary of the overpotentials performance @ 10 $mA{\cdot}cm^{-2}$ for Pt/C, $AuPt_{1/4}$, and $AuPt_{1/4Cl}$ in 1 M potassium phosphate-buffered saline (PBS, pH=7) and in 1 M potassium hydroxide (pH=14) electrolytes.

III-STABILITY TEST

Fig. S15. (a) CV curves at different scan rates (20 to 200 $mV{\cdot}s^{-1}$) for a) $AuPt_{1/4Cl}$, b) (a) commercial Pt/C and (b) $AuPt_{1/4}$.

Fig. S16. a) Chronopotentiometry for $AuPt_{1/4Cl}$ samples at 10 and 50 $mA{\cdot}cm^{-2}$ (black line/squares and orange line/circles). b) Zoom in of the 0 to 12 hours region of the chronopotentiometry.

Figure S17: Characterizations of $AuPt_{1/4Cl}$ after long term stability measurement: (a-d) TEM and HR-TEM images at different magnifications and measured lattice fingers; (e and f) EDX mapping of different NCs; and (g) Au and Pt composition along a set of NCs (EDX line scanning).

Figure S18: High resolution XPS spectra for $AuPt_{1/4Cl}$ NCs (a, b) before and (c, d) after a chronopotentiometry (200 hours at 10 $mA{\cdot}cm^{-2}$).

Table S4: Summary of the specific data published about stability measurements by running CV cycles or chronoamperometry/chronopotentiometry.

IV.-Reference

I. NCs Characterization

X-ray diffraction (XRD)

XRD patterns were collected using a conventional Cu-Kα radiation source (λ = 1.5406 Å) in a Bruker ADVANCE D8 with Bragg–Brentano geometry. Intensity was recorded in the 2θ range from 30 to 80° at a scanning step of 0.02°·s^{-1}. Samples were prepared by drop-casting and further evaporating a concentrated solution of NCs onto an amorphous silicon wafer.

Transmission electron microscope (TEM) and high-resolution scanning transmission electron microscopy (HR-STEM) analysis

Electron micrographs were obtained in a JEOL 1210 TEM operating at 120 kV, equipped with a side-entry 60°/30° double tilt GATAN 646 specimen holder. HR-STEM, high-angle annular dark-field STEM (HAADF-STEM) images and STEM-energy dispersive X-ray spectroscopy (STEM-EDX) maps were acquired using a FEI Titan microscope operated at 300 kV. Samples were prepared by drop-casting a diluted solution of NCs onto a carbon-coated Cu TEM grid (400 mesh).

Spectroscopy characterization

Ultraviolet-visible (UV-Vis) spectra were collected on a JASCO V-780 UV-Vis-NIR spectrophotometer between 200 and 800 nm. Infrared (IR) analysis was carried out in a Fourier Transform Infrared Spectroscopy (FT-IR) Jasco 4700 spectrometer in Attenuated Total Reflectance accessory (ATR) mode, covering the energy range from 300 to 7800 cm^{-1}.

Inductively coupled plasma atomic emission spectroscopy (ICP-OES)

For evaluating the final Au:Pt ratios of the NCs, ICP-OES was performed on an Agilent 5900. In order to prepare the ICP-OES solutions, samples were digested overnight by adding 100 µL NCs' solution into 1 mL of aqua regia, and the final solution was diluted to 10 mL by adding MQ-H_2O.

Fig. S1. Evolution of the NCs size and morphology as a function of time for the synthesis of $AuPt_{1/1}$. Samples were annealed at 160 °C in a solution containing a 1:1 Au:Pt molar ratio for (a) 10 s, (b) 30 s, (c) 1 min, (d) 2 min, (e) 5 min, and (f) 10 min. Scale bar =100 nm.

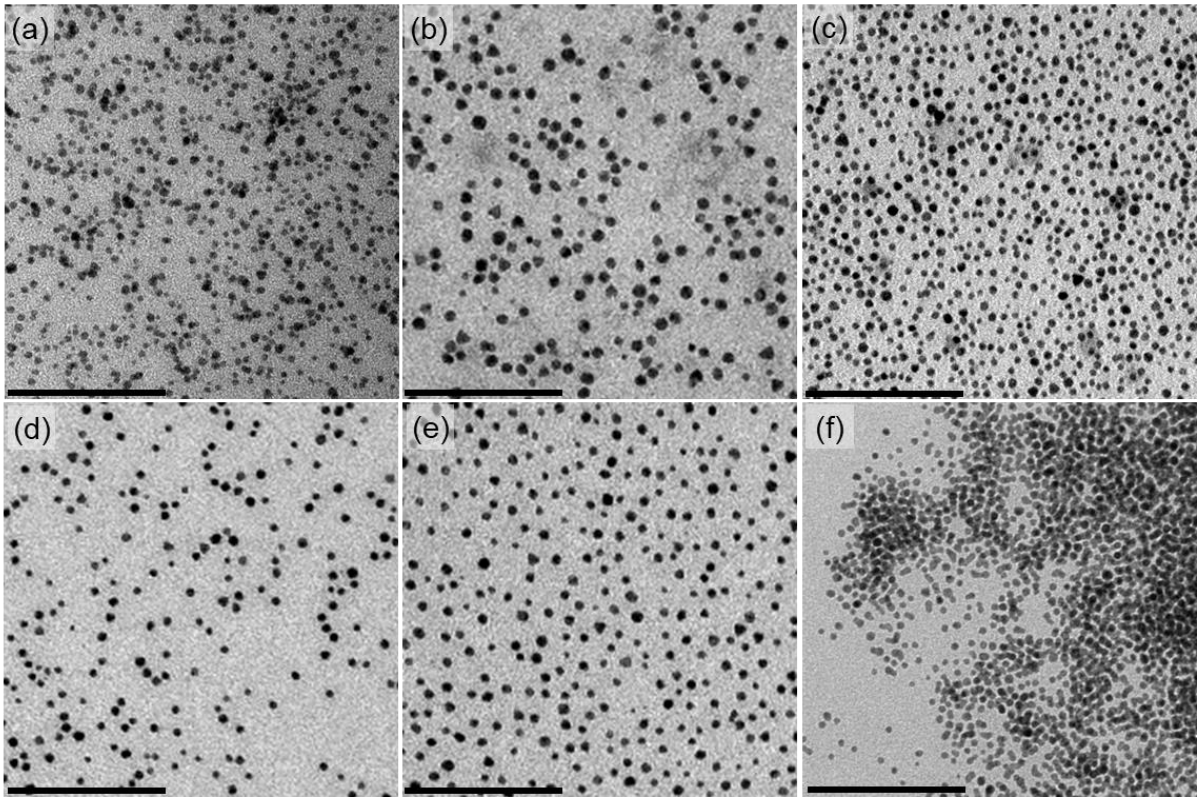

Fig. S2. Evolution of the AuPt NCs size and shape as a function of the amount of PVP_{10K} (25, 50 and 100 mg) for different Au:Pt ratios (1:0 a-c; 1:4 d-f; 1:1 g-I; 1:0 j-k). Scale bar = 100 nm.

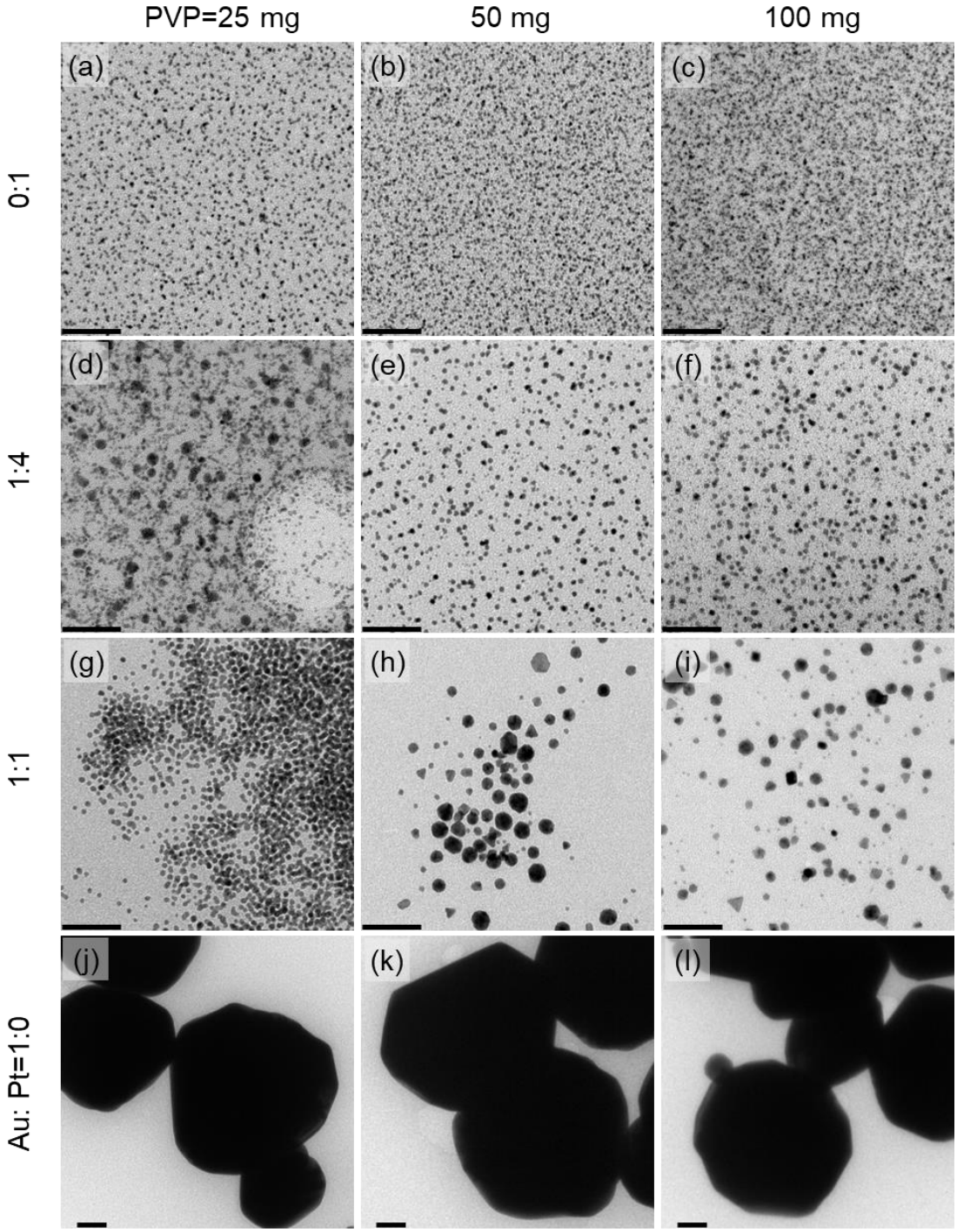

Fig. S3. Evolution of the size and shape for AuPt NCs as a function of the total metal concentration (Au + Pt).

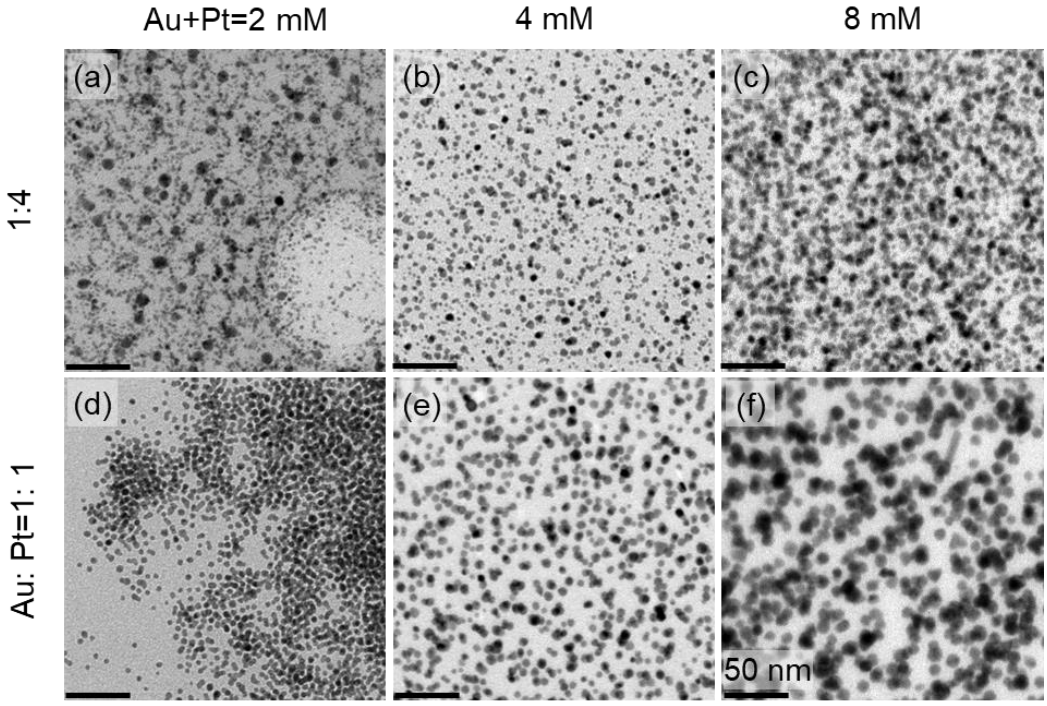

Fig. S4. XRD and UV-Vis patterns for AuPt NCs synthesized at different Au:Pt ratios without ($Au:Pt_{x/y}$; a, b) and with ($Au:Pt_{x/yCl}$ c, d) HCl.

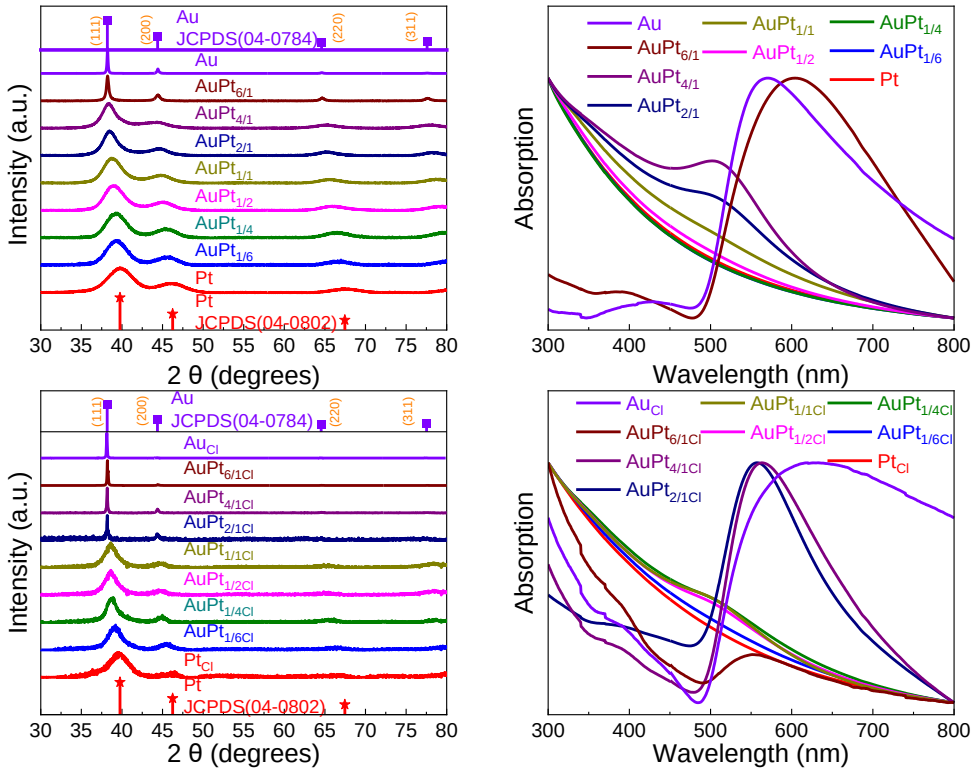

Fig. S5. a) Comparison between the final Pt amount inside the NCs evaluated by ICP-OES (Pt_{ICP} in %) and the Pt amount added in solution ($Pt_{feeding}$ in %) for samples prepared under standard conditions (open blue circles) and in the presence of an excess of chlorine ions (green crosses). b) Evaluation of the difference in Pt content (ΔPt) between samples prepared with and without excess chlorine ions as a function of Pt content in the reaction solution ($Pt_{feeding}$ in %). The yellow area corresponds to the Pt % for the 1:6 to 1:2 Au:Pt ratio range.

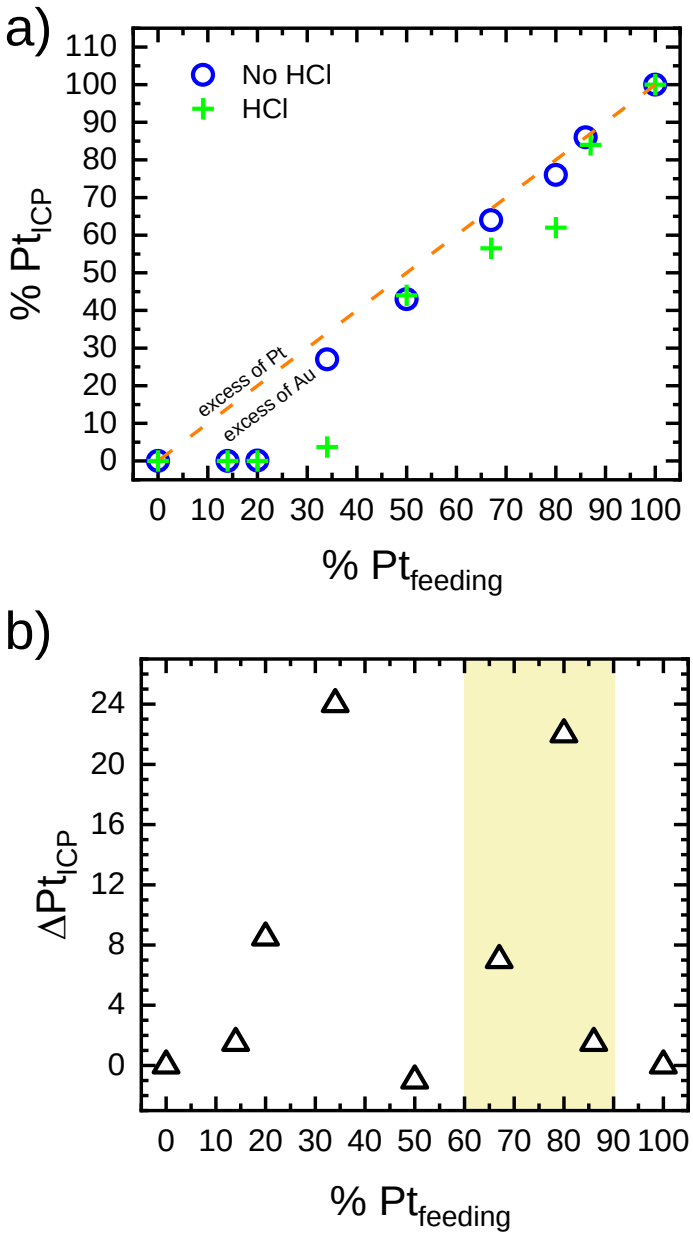

Fig. S6. Size and shape evolution of AuPt NCs produced at different Au:Pt ratios (0:1 a-d; 1:4 e-h; 1:1 i-l; and 1:0: m-p) under different amounts of chlorine ions (0, 10, 20 and 50 µL of a 37 wt% HCl solution). Scale bar = 50 nm.

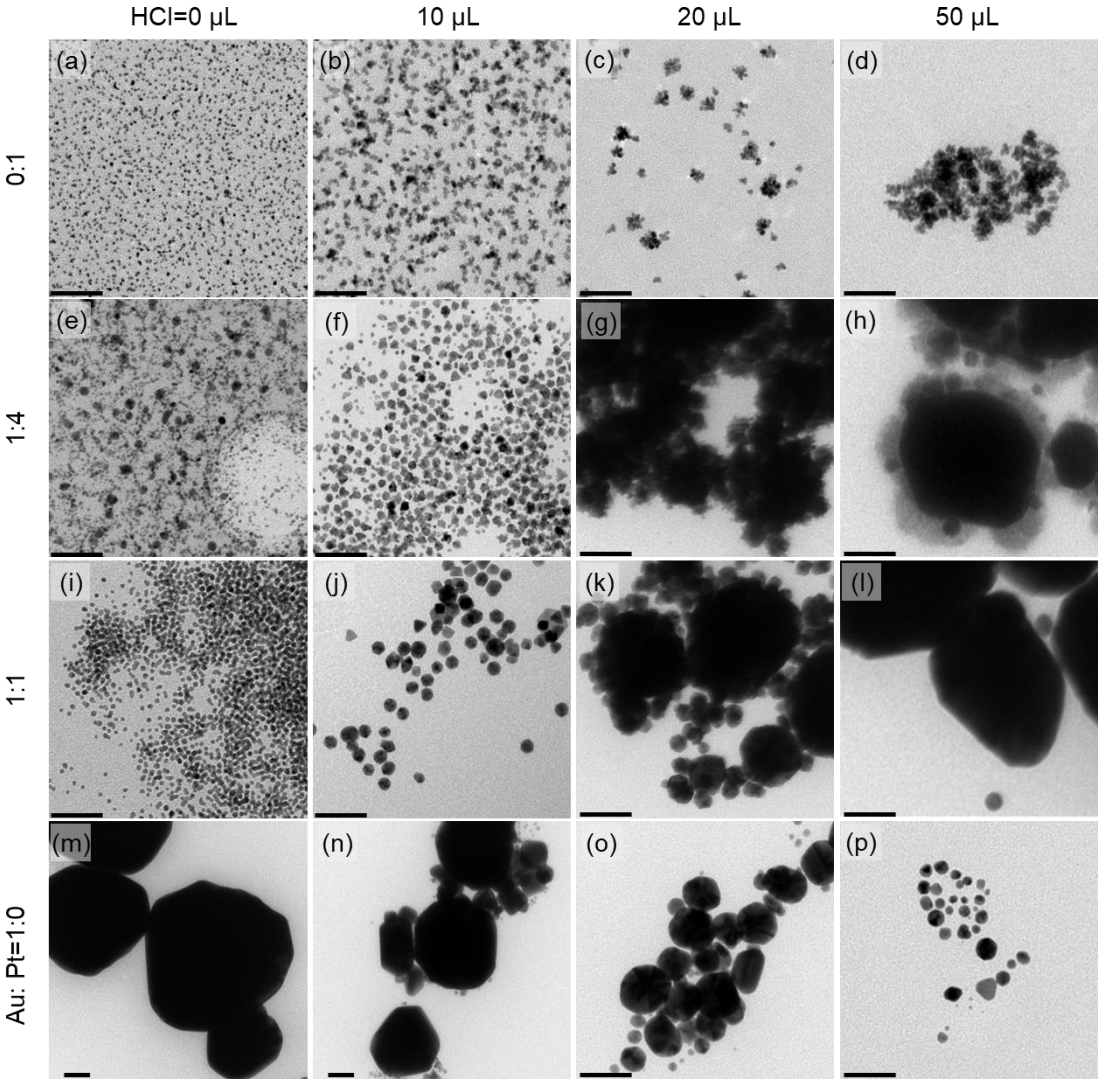

Fig. S7. Size and shape evolution as a function of PVP_{10k} amount (25, 50 and 100 mg) for AuPt NCs produced in the presence of 10 µL of chlorine ions. Scale bar = 50 nm.

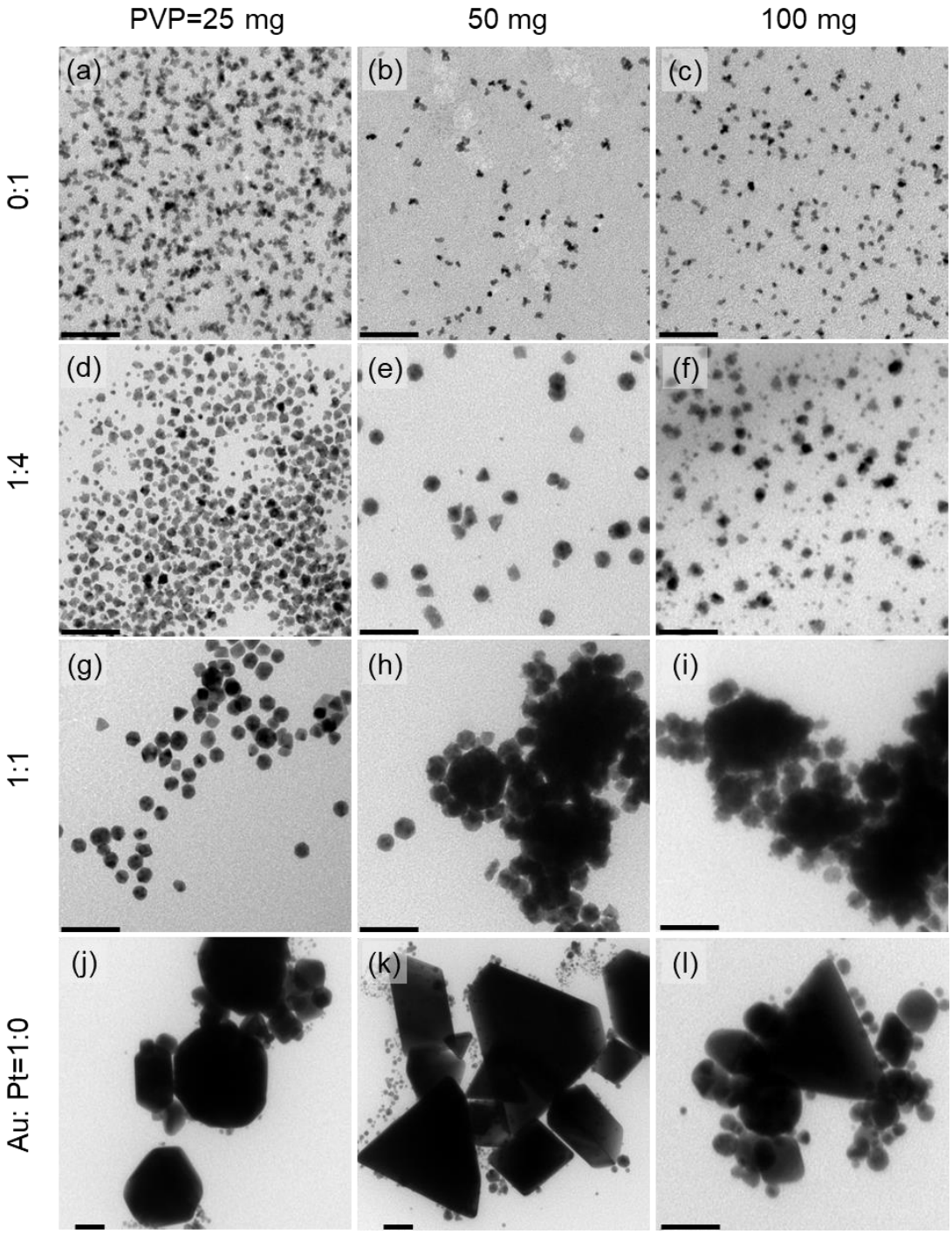

Fig. S8. TEM images for AuPt NCs synthesized at 1:4 (a-c) and 1:1 (d-f) rations but increasing total metal concertation (2, 4 and 8 mM). In the reaction solution, 10 µL of an HCl solution (37 wt%) were added deliberately to increase the amount of chlorine ions. Scale bar = 50 nm.

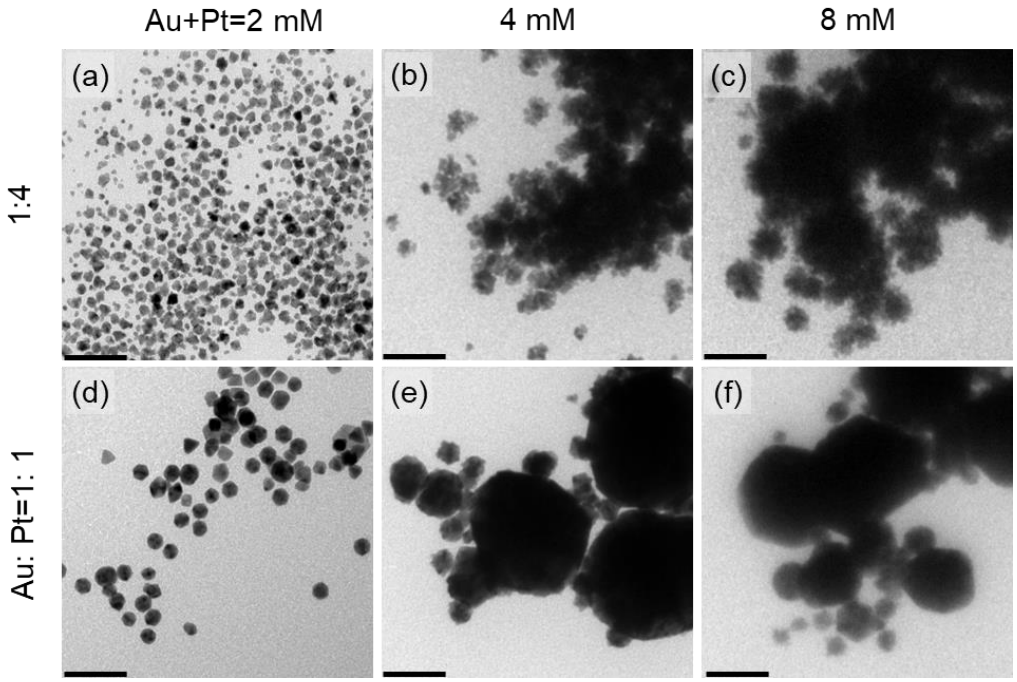

Fig. S9. Direct comparison of AuPt NCs produced with a 1:1 Au:Pt molar ratio without or with HCl using a MW-assisted approach for 10 min (a, d) or an oil bath for 10 min (b, e) and 60 min. (c, f). Scale bar = 50 nm.

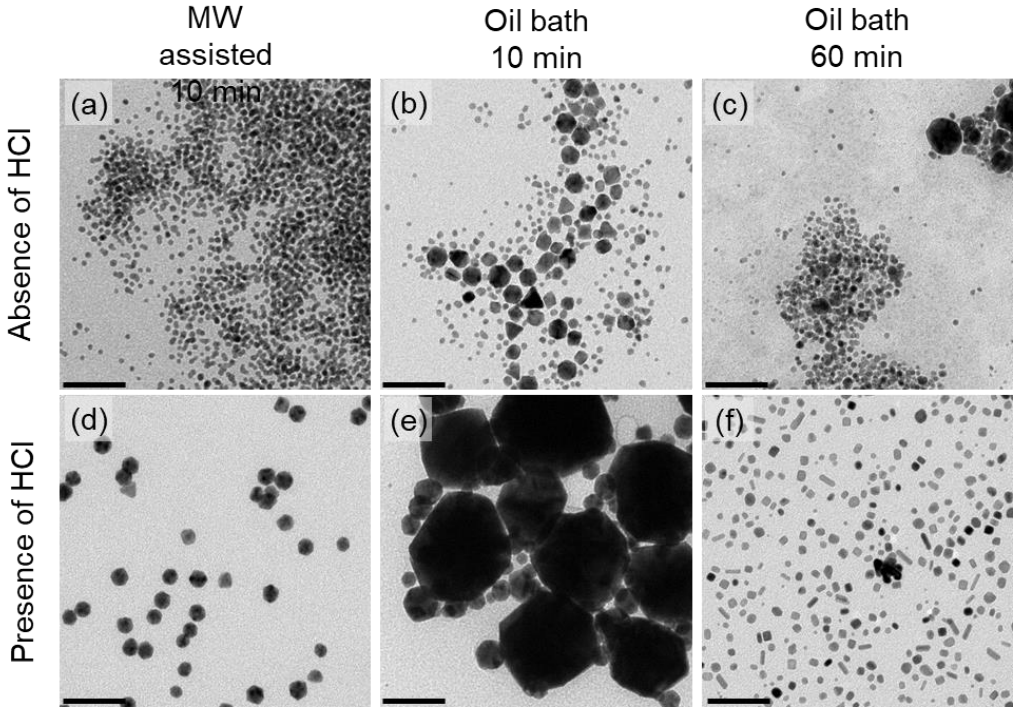

Fig. S10. a-c) TEM images of the NCs produced in three different experiments but under the same reaction conditions ($AuPt_{1/4Cl}$). d) TEM image of NCs produced after scaling up the reaction condition from 4 to 70 mL (17.5-fold). The final volume was the maximum possible achieved using the flexiWAVE reactor (Milestone™ Srl).

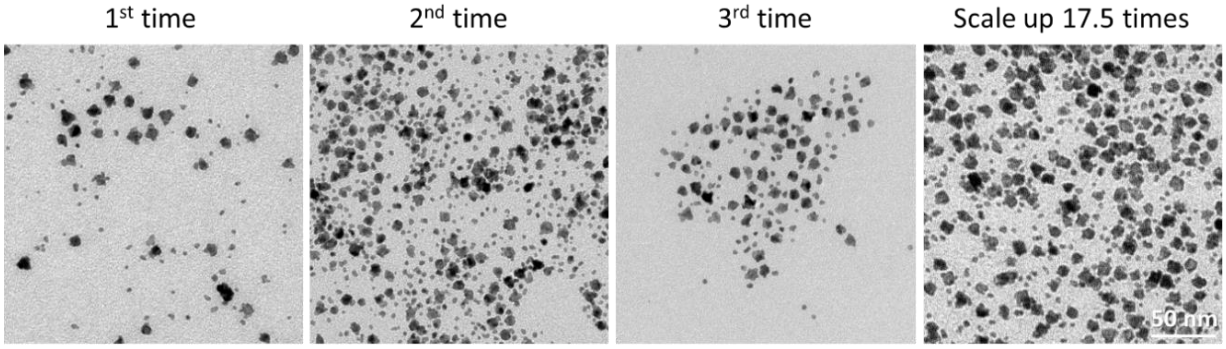

Fig. S11. FT-IR pattern of pure PVP_{10k}, $AuPt_{1/1}$ before and after PVP_{10k} removal.

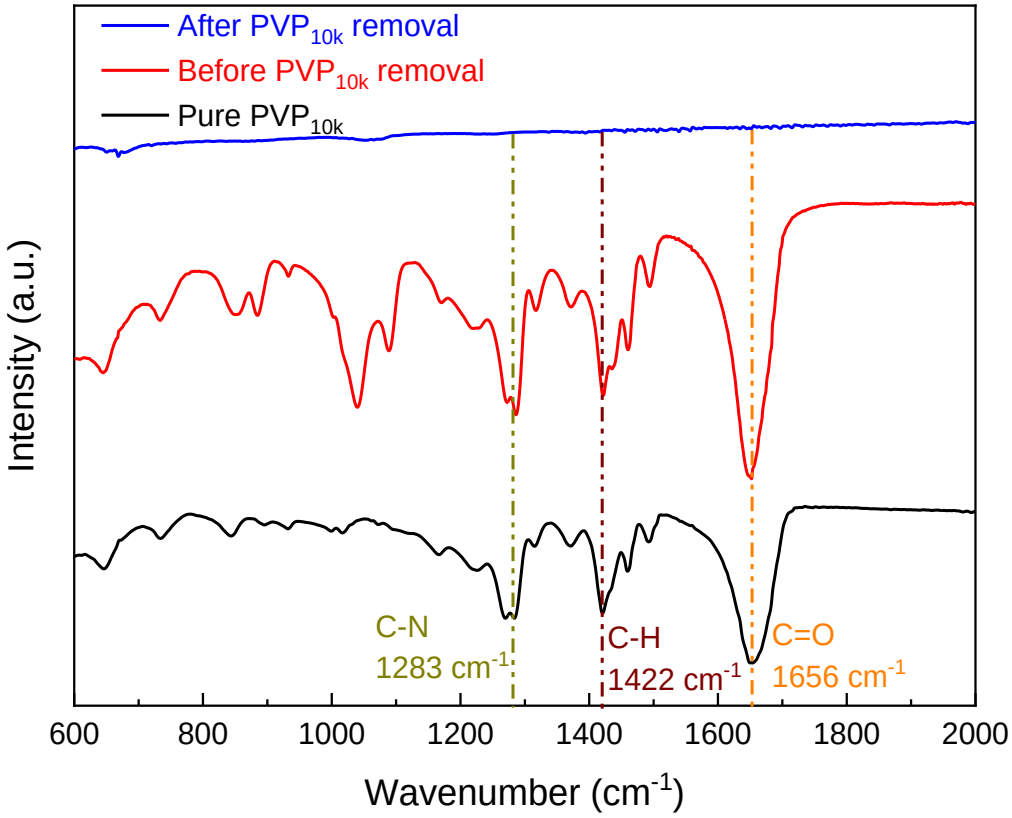

Fig.S12. Electrocatalytic HER performance in 0.5 M H_2SO_4. LSV of the AuPt NCs synthesized in the absence (a) or presence (b) of chlorine without IR. (c) Comparison of the LSV with and without IR compensation (dashed and solid lines, respectively) for $AuPt_{1/4}$ and $AuPt_{1/4Cl}$ samples.

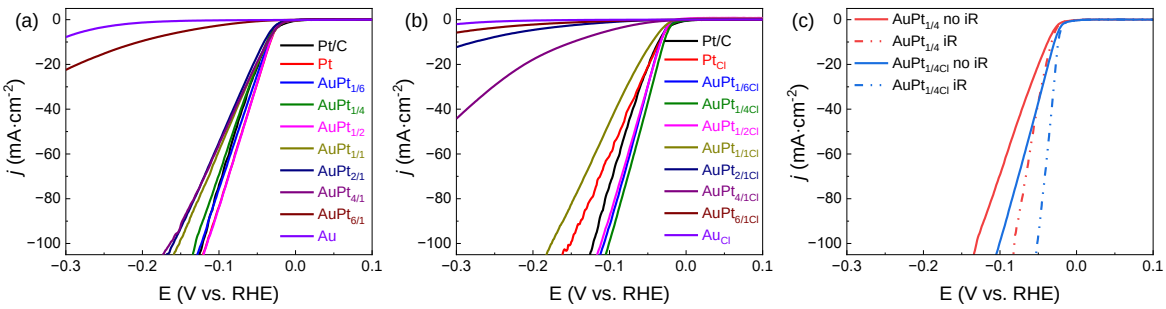

Fig. S13. Magnification of the Nyquist plot reported in Fig. 3h along with the equivalent circuit model.

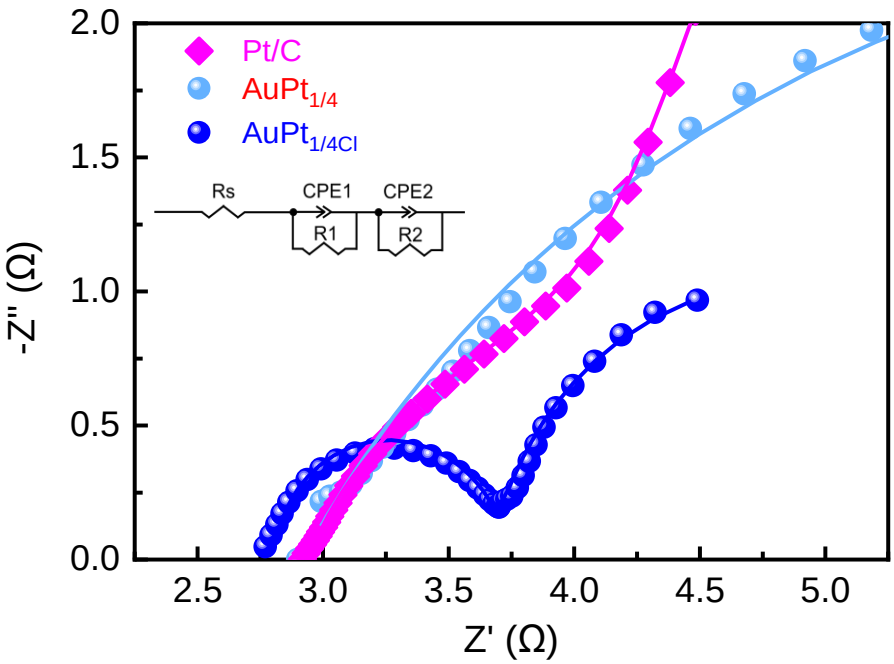

Table S1. Summary of the specific data of the references cited in Fig. 3g.

Sample	Tafel slope ($mV \cdot dec^{-1}$)	Overpotential @ 10 $mA \cdot cm^{-2}$ (mV)	References
$AuPt_{1/4Cl}$	13	24	This work
$AuPt_{1/4}$	26	32	
Pt/C	30	31	
PtAu/rGO	38	50	[1]
AuPt NDs	34	48	[2]
AuPtPd NDs	36	29	[3]
$Pt_{1.88}$-PVA	31	34	[4]
SA-Pt/MoS_2	34.83	44	[5]
Pt(110)-Ni_3N	44.9	33	[6]
Pt-ACs/CoNC	29.8	42	[7]
PtNPs/3DHPNG/Aupla/GCE	25.2	10	[8]
USCS $Au_{38.4}$@$Au_{9.3}Pt_{52.3}$-NP/C	14	16	[9]
Pt/NBF-ReS_2/Mo_2CT_x	24	29	[10]
PtW_6O_{24}/C	29.8	22	[11]
Pt/P@Cu	50.2	24.3	[12]
$PtHCu_{11}$ (2)	39	30	[13]
Pt_5/HMCS-5.08%	28.3	20.7	[14]
Pt_1/NMHCS	24	40	[15]

Table S2. Summary of the parameters obtained from the RC equivalent circuit model.

Sample	Potential (V vs. RHE)	R_s (Ω)	R_1 (Ω)	R_2 (Ω)	CPE_1	CPE_2
$AuPt_{1/4Cl}$	-0.013	2.80	0.87	2.40	0.0137	0.9228
$AuPt_{1/4}$	-0.013	2.88	6.34	9.24	0.0138	0.8017
Pt/C	-0.013	2.94	1.54	17.04	0.0037	0.9867

S2: HER measurement in neutral and alkaline media

Reagents: Phosphate buffered saline (PBS) was purchased from Sigma-Aldrich. Potassium hydroxide (KOH, 85%) was purchased from Fisher Scientific.

The measurement in neutral electrolyte consisted in 1M PBS solution adjusted to pH=7 with 30-min Ar bubbling. In the system, a grassy carbon electrode (5 mm in diameter) acted as the working electrode (WE), a graphite electrode acted as the counter electrode (CE) and a Ag/AgCl electrode acted as the reference electrode (RE) for HER. The amount of catalyst used was the same as the measurement in acidic electrolyte. All potentials were corrected to the reversible hydrogen electrode (RHE) by the following equation: $E_{RHE} = E_{Ag/AgCl} + 0.0591\ pH + 0.197\ V$.

The measurement in alkaline electrolyte consisted in 1 M KOH solution at pH=14 with 30-min Ar bubbling. In the system, a grassy carbon electrode (5 mm in diameter) acted as the WE, a graphite electrode acted as the CE and a Hg/HgO electrode acted as the RE for HER. The amount of catalyst used was the same as the measurement in acidic electrolyte. All potentials were corrected to the reversible hydrogen electrode (RHE) by the following equation: $E_{RHE} = E_{Hg/HgO} + 0.0591\ pH + 0.098\ V$.

The polarization curves were obtained with a scan rate of 5 $mV \cdot s^{-1}$, which were all corrected for the 90% iR compensation within the cell.

Fig. S14. LSV curves of Pt/C, $AuPt_{1/4}$, and $AuPt_{1/4Cl}$ in (a) 1 M potassium phosphate-buffered saline (PBS, pH=7) electrolyte and (b) 1 M potassium hydroxide (pH=14) electrolyte.

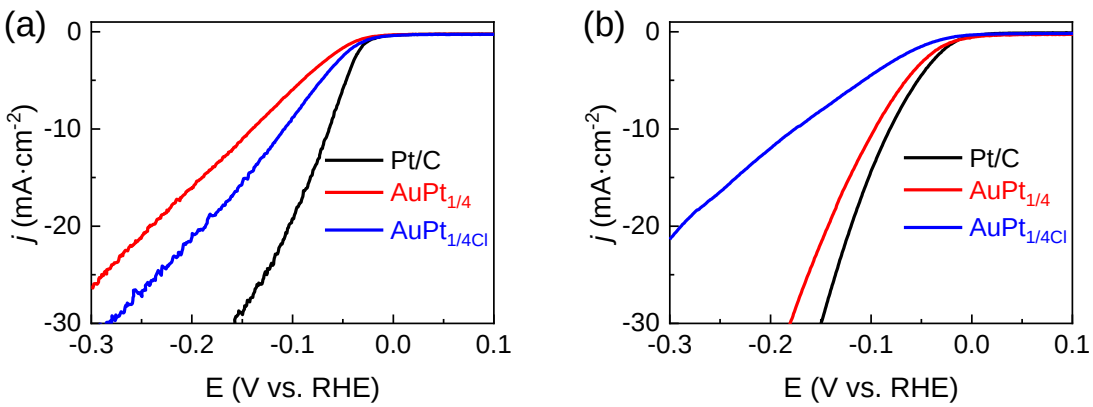

Table S3. Summary of the overpotentials performance @ 10 mA·cm^{-2} for Pt/C, $AuPt_{1/4}$, and $AuPt_{1/4Cl}$ in 1 M potassium phosphate-buffered saline (PBS, pH=7) and in 1 M potassium hydroxide (pH=14) electrolytes.

Samples	**Overpotentials at 10 mA·cm^{-2} (mV)**	
	Potassium phosphate-buffered (pH = 7)	Potassium hydroxide (pH = 14)
Pt/C	64	81
$AuPt_{1/4}$	140	96
$AuPt_{1/4Cl}$	108	176

S3: Stability test

Chronopotentiometry measurements: For the stability test of $AuPt_{1/4Cl}$, the chronopotentiometry curve was obtained at a current density of 10 and 50 mA·cm^{-2} in 0.5 M H_2SO_4 using an H-type cell with Fumasep FAA-3-50 anion exchange membrane AEM. The WE was prepared by drop casting 375 µL·of the catalyst ink (see experimental section) onto a carbon cloth (1 x 1.25 cm^2).

Fig. S15. (a) CV curves at different scan rates (20 to 200 mV·s^{-1}) for a) $AuPt_{1/4Cl}$, b) commercial Pt/C and c) $AuPt_{1/4}$.

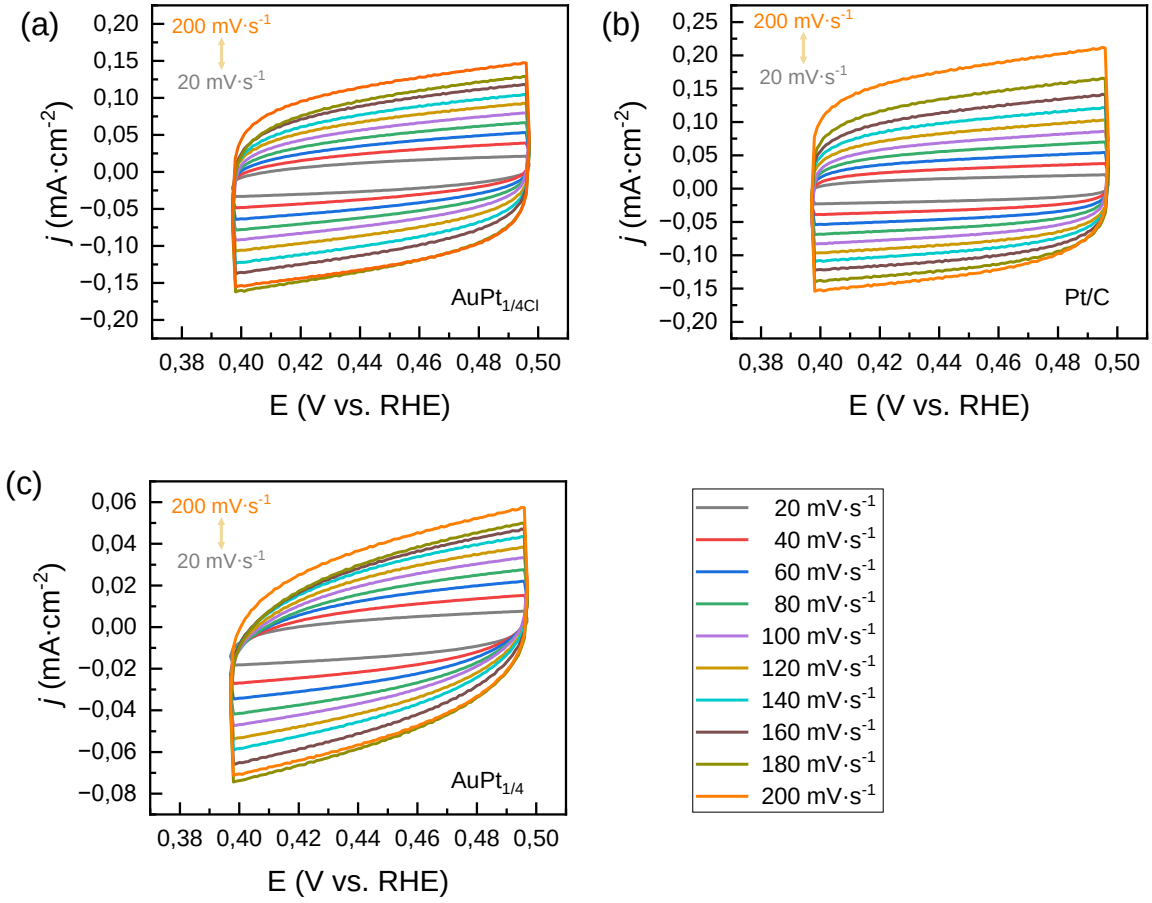

Fig. S16. a) Chronopotentiometry for $AuPt_{1/4Cl}$ samples at 10 and 50 mA·cm^{-2} (black line/squares and orange line/circles). b) Zoom in of the 0 to 12 hours region of the chronopotentiometry.

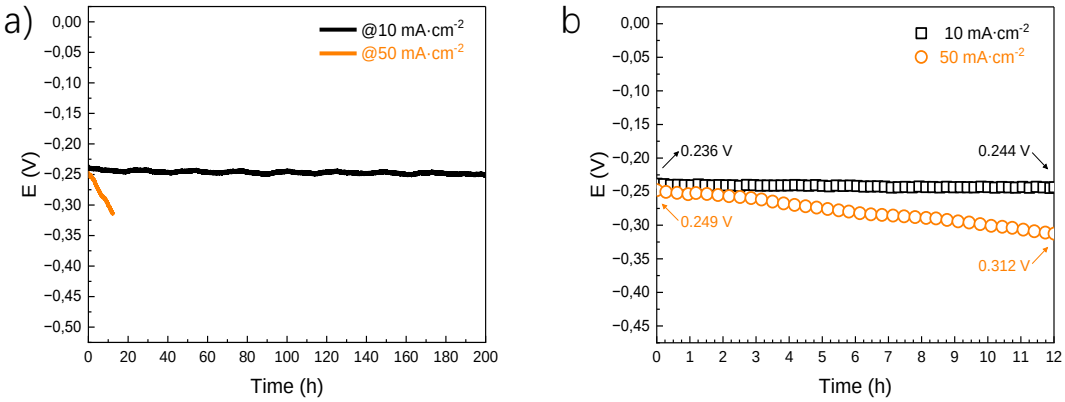

Figure S17: Characterizations of $AuPt_{1/4Cl}$ after long term stability measurement: (a-d) TEM and HR-TEM images at different magnifications and measured lattice fingers; (e and f) EDX mapping of different NCs; and (g) Au and Pt composition along a set of NCs (EDX line scanning).

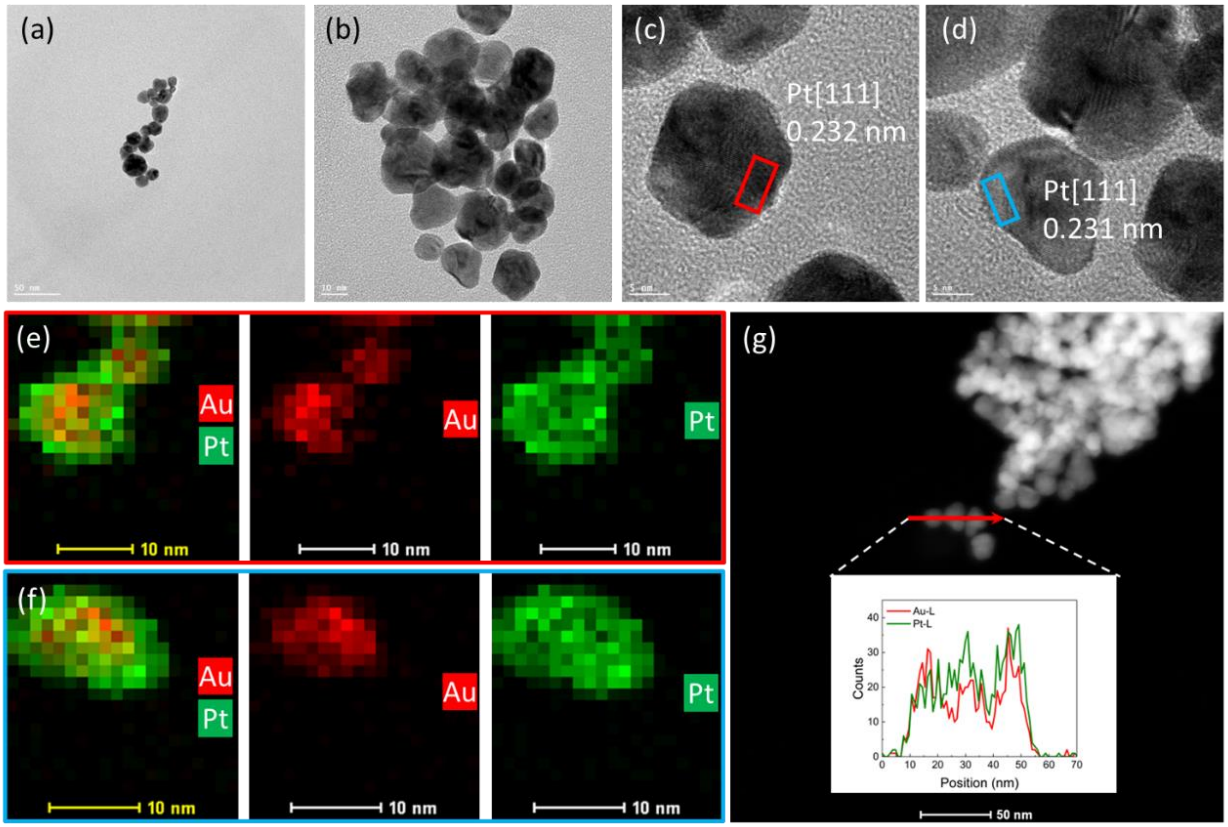

Figure S18: High resolution XPS spectra for $AuPt_{1/4Cl}$ NCs (a, b) before and (c, d) after a chronopotentiometry (200 hours at 10 mA·cm^{-2}).

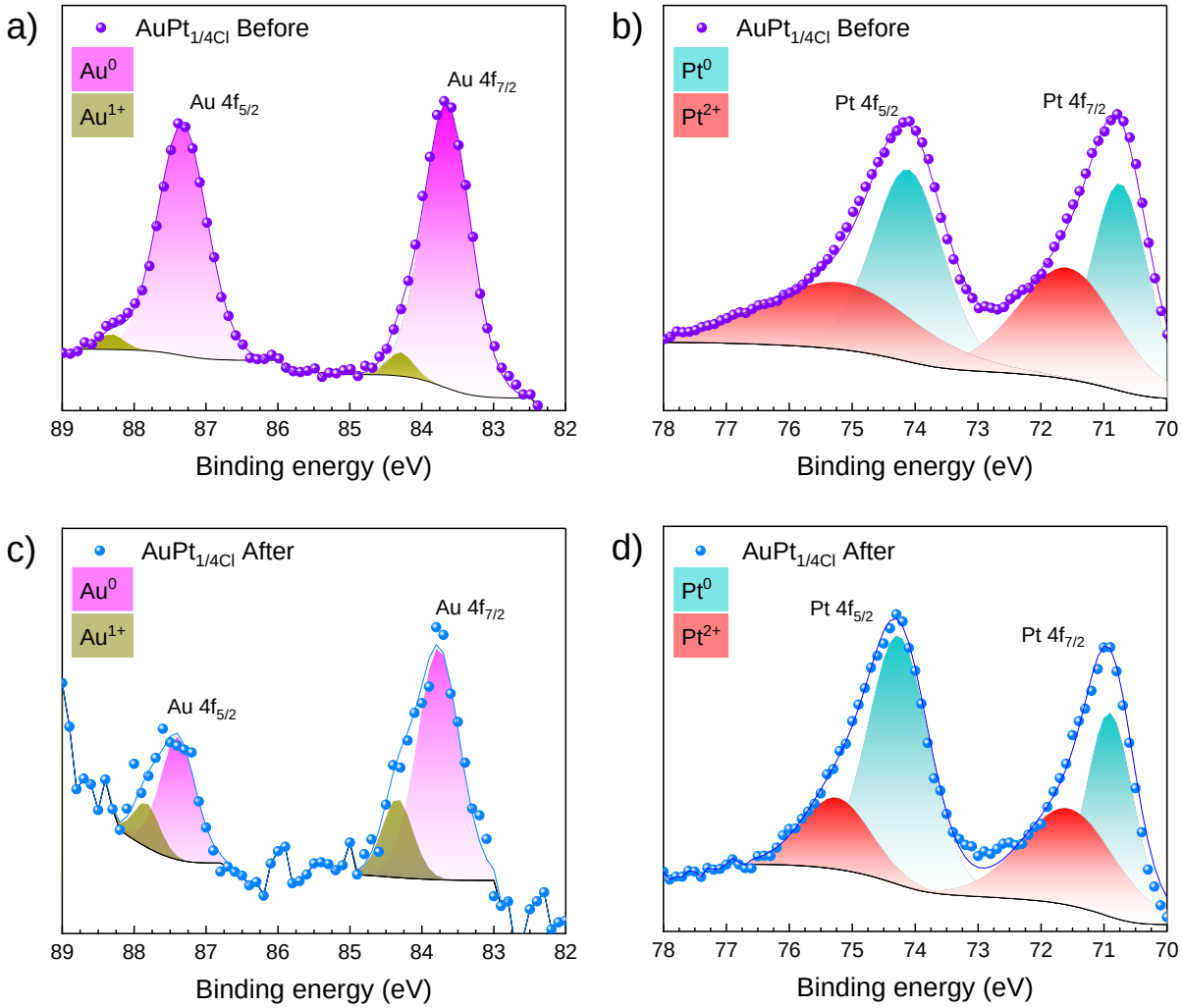

Table S4: Summary of the specific data published about stability measurements by running CV cycles or chronoamperometry/chronopotentiometry.

Sample	**CV cycles (times)**	**Chronoamperometry/Chronopotentiometry @10 mA·cm^{-2} (h)**	**References**
$AuPt_{1/4Cl}$	4000	200	This work
Pt5/HMCS-5.08%	3000	5.56	[16]
Pt1/NMHCS	3000	10	[17]
$CoSe_2$/a-CoP	-	50	[18]
Pd NPs-Bis-24h	10000	40	[19]
MoP-Ru2P/NPC	-	12	[20]
E-MoS2-Pt-r	1000	10	[21]
AuPtPd NPs	1000	2.78	[22]
Pt-ACs/CoNC	5000	50	[23]
Pt(110)-Ni3N	-	24	[24]
CB[8]-Pt	10000	120	[25]
Pt/P@Cu	1000	20h @20 mA·cm^{-2}	[26]
PtHCu11 (2)	3000	-	[27]

References

1 L. Rakočević, I. S. Simatović, A. Maksić, V. Rajić, S. Štrbac and I. Srejić, *Catalysts*, , DOI:10.3390/catal12010043.

2 J. J. Feng, L. Liu, X. Ma, J. Yuan and A. J. Wang, *Int J Hydrogen Energy*, 2017, **42**, 2071–2080.

3 H. Y. Chen, A. J. Wang, L. Zhang, J. Yuan, Q. L. Zhang and J. J. Feng, *Int J Hydrogen Energy*, 2018, **43**, 22187–22194.

4 Y. Qu, Z. Yu, D. Wei, L. Chen, Z. Zheng, N. Xiao, L. Wang and J. Yu, *Ionics (Kiel)*, 2021, **27**, 4885–4895.

5 J. Zhu, Y. Tu, L. Cai, H. Ma, Y. Chai, L. Zhang and W. Zhang, *Small*, , DOI:10.1002/smll.202104824.

6 S. Qiao, Q. He, Q. Zhou, Y. Zhou, W. Xu, H. Shou, Y. Cao, S. Chen, X. Wu and L. Song, *Nano Res*, 2023, **16**, 174–180.

7 Y. Zhao, P. V. Kumar, X. Tan, X. Lu, X. Zhu, J. Jiang, J. Pan, S. Xi, H. Y. Yang, Z. Ma, T. Wan, D. Chu, W. Jiang, S. C. Smith, R. Amal, Z. Han and X. Lu, *Nat Commun*, , DOI:10.1038/s41467-022-30155-4.

8 Y. Zhang, L. Liu, C. Sun, Y. Du, Y. Zhou and Q. Xie, *J Alloys Compd*, , DOI:10.1016/j.jallcom.2021.161564.

9 Y. Cao, Y. Xiahou, L. Xing, X. Zhang, H. Li, C. S. Wu and H. Xia, *Nanoscale*, 2020, **12**, 20456–20466.

10 M. Yi, N. Li, B. Lu, L. Li, Z. Zhu and J. Zhang, *Energy Storage Mater*, 2021, **42**, 418–429.

11 F. Y. Yu, Z. L. Lang, L. Y. Yin, K. Feng, Y. J. Xia, H. Q. Tan, H. T. Zhu, J. Zhong, Z. H. Kang and Y. G. Li, *Nat Commun*, , DOI:10.1038/s41467-019-14274-z.

12 Y. Tan, L. Liu, L. Zhang, S. Zhao, D. J. L. Brett, P. R. Shearing, Y. Bai, I. P. Parkin and G. He, *Mater Adv*, 2022, **3**, 7667–7672.

13 R. P. Brocha Silalahi, H. Liang, Y. Jo, J. H. Liao, T. H. Chiu, Y. Y. Wu, X. Wang, S. Kahlal, Q. Wang, W. Choi, D. Lee, J. Y. Saillard and C. W. Liu, *Chemistry - A European Journal*, , DOI:10.1002/chem.202303755.

14 X. K. Wan, H. Bin Wu, B. Y. Guan, D. Luan and X. W. Lou, *Advanced Materials*, , DOI:10.1002/adma.201901349.

15 P. Kuang, Y. Wang, B. Zhu, F. Xia, C. W. Tung, J. Wu, H. M. Chen and J. Yu, *Advanced Materials*, , DOI:10.1002/adma.202008599.

16 X. K. Wan, H. Bin Wu, B. Y. Guan, D. Luan and X. W. Lou, *Advanced Materials*, , DOI:10.1002/adma.201901349.

17 P. Kuang, Y. Wang, B. Zhu, F. Xia, C. W. Tung, J. Wu, H. M. Chen and J. Yu, *Advanced Materials*, , DOI:10.1002/adma.202008599.

18 S. Shen, Z. Wang, Z. Lin, K. Song, Q. Zhang, F. Meng, L. Gu and W. Zhong, *Advanced Materials*, , DOI:10.1002/adma.202110631.

19 H. Cheng, N. Yang, G. Liu, Y. Ge, J. Huang, Q. Yun, Y. Du, C. J. Sun, B. Chen, J. Liu and H. Zhang, *Advanced Materials*, , DOI:10.1002/adma.201902964.

20 Y. Gao, Z. Chen, Y. Zhao, W. Yu, X. Jiang, M. He, Z. Li, T. Ma, Z. Wu and L. Wang, *Appl Catal B*, , DOI:10.1016/j.apcatb.2021.120879.

21 S. He, Y. Liu, H. Li, Q. Wu, D. Ma, D. Gao, J. Bi, Y. Yang and C. Cui, *ACS Appl Mater Interfaces*, 2021, **13**, 13311–13318.

22 H. Y. Chen, A. J. Wang, L. Zhang, J. Yuan, Q. L. Zhang and J. J. Feng, *Int J Hydrogen Energy*, 2018, **43**, 22187–22194.

23 Y. Zhao, P. V. Kumar, X. Tan, X. Lu, X. Zhu, J. Jiang, J. Pan, S. Xi, H. Y. Yang, Z. Ma, T. Wan, D. Chu, W. Jiang, S. C. Smith, R. Amal, Z. Han and X. Lu, *Nat Commun*, , DOI:10.1038/s41467-022-30155-4.

24 S. Qiao, Q. He, Q. Zhou, Y. Zhou, W. Xu, H. Shou, Y. Cao, S. Chen, X. Wu and L. Song, *Nano Res*, 2023, **16**, 174–180.

25 W. Geng, X. Song, Z. Wei, M. Cao and R. Cao, *ACS Appl Energy Mater*, 2022, **5**, 15597–15604.

26 Y. Tan, L. Liu, L. Zhang, S. Zhao, D. J. L. Brett, P. R. Shearing, Y. Bai, I. P. Parkin and G. He, *Mater Adv*, 2022, **3**, 7667–7672.

27 R. P. Brocha Silalahi, H. Liang, Y. Jo, J. H. Liao, T. H. Chiu, Y. Y. Wu, X. Wang, S. Kahlal, Q. Wang, W. Choi, D. Lee, J. Y. Saillard and C. W. Liu, *Chemistry - A European Journal*, , DOI:10.1002/chem.202303755.